European Journal of Soil Science, February 2008, **59,** 103–113 doi: 10.1111/j.1365-2389.2007.00974.x

Analysing flow patterns from dye tracer experiments in a forest soil using extreme value statistics

C. BOGNER[a], B. WOLF[a], M. SCHLATHER[b] & B. HUWE[a]
[a]*Soil Physics Group, University of Bayreuth, 95440 Bayreuth, Germany, and* [b]*Institute for Mathematical Stochastics, Georgia Augusta University Göttingen, Maschmühlenweg 8-10, 37073 Göttingen, Germany*

Summary

Preferential flow of water in soil is now recognized as a common phenomenon. It results in complex flow patterns that can be visualized by dye tracers and increases the risk of pollutants reaching greater depths. We analysed the behaviour of a risk index for vertical solute propagation based on extreme value theory. This risk index can be calculated from binary images of dye-stained soil profiles and is defined as the form parameter of the generalized Pareto distribution. We did five tracer experiments with Brilliant Blue and iodide under changing initial (variable initial soil moisture) and experimental conditions (different irrigation rates). Our results indicate some persistence of the risk index against small changes of experimental conditions such as the irrigation rate. On the other hand, it seems to be affected by initial soil moisture. Comparisons of Brilliant Blue and iodide patterns show that the form parameter alone is not sufficient to estimate the risk of vertical solute propagation. Therefore we propose to combine the risk index with the scale parameter of the generalized Pareto distribution.

Introduction

Although preferential flow of water in soil was discovered in the late 19th century (Schumacher, 1864; Lawes *et al*., 1882), it was considered for a long time as exceptional. Today, it is regarded as a common phenomenon that depends on the spatial heterogeneity and intensity of rainfall (Gish *et al*., 2004), water repellency (Hendrickx *et al*., 1993; Ritsema & Dekker, 2000; Wang *et al*., 2000), soil structure (Flury *et al*., 1994; Kulli *et al*., 2003; Vogel *et al*., 2006) and biological factors such as the distributions of roots (Mitchell *et al*., 1995) and earthworm burrows (Farenhorst *et al*., 2000; Shuster *et al*., 2002; Weiler & Naef, 2003). Preferential flow results in complex flow patterns that can be visualized by dye tracers. Brilliant Blue is frequently used in vadose zone hydrology for such tracing studies, although its adsorption behaviour is non-linear and depends on soil properties (Ketelsen & Meyer-Windel, 1999; German-Heins & Flury, 2000; Kasteel *et al*., 2002). However, it is readily seen against most soil colours and has acceptable toxicological characteristics for environmental use (Flury & Flühler, 1994; Mon *et al*., 2006).

Usually, the main information obtained from dye-stained profiles is binary images – photographs of soil profiles that are classified in stained (black) and unstained (white) parts. They are used for qualitative description of flow regimes and for the visualization of preferential flow (Öhrstöm *et al*., 2002; Kulli *et al*., 2003; Weiler & Naef, 2003). Recent studies, however, took a quantitative approach to tracer studies in soils by establishing dye concentration maps (Aeby *et al*., 1997; Forrer *et al*., 1999, 2000). This method needs calibration because the same dye concentration has different hues depending on soil colour. Forrer *et al*. (2000) reported 203 calibration samples in a 'fairly uniform Eutric Cambisol' on an agricultural field. Morris & Mooney (2004) used 100 samples to assess concentrations in a small intact soil block (200 mm × 200 mm × 200 mm).

Such a calibration becomes complicated for soils with progressively changing colours because the number of calibration samples increases rapidly. This is the case at our study site. Indeed, we can distinguish four or five different main hues in our soil and varying degrees of their combinations. Each of these hues needs its own calibration between the possible concentration range of Brilliant Blue and the resulting RGB (Red, Green and Blue) values on images. Therefore, we needed some other approach to obtain quantitative information on flow processes from stained profiles, one that does not require any information on dye concentrations in the soil. Schlather & Huwe (2005) propose a risk index for groundwater vulnerability to pollutants based on extreme value theory. It can be calculated from binary images of dye-stained soil profiles and does not require any

Correspondence: C. Bogner. E-mail: christina.bogner@uni-bayreuth.de
Received 31 January 2007; revised version accepted 13 September 2007

additional information on soil properties. The goal of our study is to consider in detail the behaviour of the risk index for different experimental and initial conditions.

Materials and methods

Dye tracer experiments

We did five tracer experiments in a Norway spruce forest in southeast Germany. The soil is a Cambisol or a Cambic Podzol with loam or sandy loam above loamy sand. The stone content is highly variable, and the pH is 4-5. We used Brilliant Blue FCF and iodide as tracers. The latter served as reference because Brilliant Blue may be retarded with regard to infiltrating water as a result of adsorption on soil particles. Bowman (1984) reported that the sorption behaviour of iodide is similar to that of bromide, which is considered as the most suitable tracer for water movement in soil (Flury & Wai, 2003). In order to have the same spatial resolution of flow patterns for both tracers, we visualized iodide by a spray method proposed by Lu & Wu (2003). Following this we applied a solution of iron(III) nitrate and starch directly on the excavated soil profile. Iron(III) oxidized iodide to iodine, which formed a dark-blue complex with starch. This method worked well; however, the time reported by Lu & Wu (2003) of about 1–2 hours for the colour reaction was not sufficient for a good contrast to Brilliant Blue dye, and we let it develop during the night. Lu & Wu (2003) also proposed a visualization method for bromide, but the Prussian blue complex formed has a blue colour that would be too difficult to distinguish from Brilliant Blue.

We applied 64 mm of tracer solution on plots of about 2 m^2 using a sprinkler similar to that proposed by Ghodrati *et al.* (1990). The irrigation rate was either 32 mm $hour^{-1}$ (referred to as 'low') or 64 mm $hour^{-1}$ ('high'), and the concentration of both tracers in the solution was 5 g l^{-1}. The maximum 10-minutes intensity recorded at the study site between 1999 and 2006 was 22 mm and the maximum 1-hour intensity was 54 mm. So the applied irrigation rate was fairly high but not unrealistic. Before the experiment, plots 1 and 2 were covered for approximately 2 weeks and are referred to as 'moist'; plots 4 and 5 were covered for approximately 5 weeks and are called 'dry'. The initial matric potential before the plots were covered was −157 hPa at 0.2 m, −53 hPa at 0.3 m and −14 hPa at 1.0 m depth. Plot 3 was not covered and represented the actual field moisture conditions of the study site. Here, the matric potential before tracer application was −52 hPa at 0.2 m, −46 hPa at 0.3 m and −25 hPa at 1.0 m depth. Plot 2 was additionally irrigated with 64 mm of water just before tracer application. Prior to irrigation, we removed the spruce cones as they covered a large portion of the soil surface, but left the litter untouched. Table 1 summarizes the experimental boundary conditions.

The day after the irrigation, six vertical 1 m × 1 m soil profiles were excavated at intervals of 20 cm in the central part of the plot. We lit them by halogen projectors to supplement the natural daylight in the forest and photographed them with a CCD camera in RAW format. In this lossless format the image is not processed by the camera software and must be transformed in JPEG or TIFF by appropriate graphics software. Thus finer control is gained over white balance, sharpness or colour space. A rectangular frame and a grey scale were placed around the profiles for later correction of distortion and white balance adjustment. Soil samples were taken for texture analysis in the laboratory, and Figure 1 summarizes the results. Nine profiles (one, two or three per plot) were treated with the indicator solution of iron(III) nitrate and starch to visualize iodide. They were photographed the same way as Brilliant Blue patterns.

Table 1 Experimental conditions for dye tracer experiments

Plot	Initial moisture	Irrigation rate/mm $hour^{-1}$
1	'Moist'[a]	64
2	'Moist'	64[b]
3	'Natural'[c]	64
4	'Dry'[d]	64
5	'Dry'	32

[a]Covered for approximately 2 weeks.
[b]Pre-irrigated with 64 mm of water just before tracer application.
[c]Not covered.
[d]Covered for approximately 5 weeks.

In some sections of plot 3, large blocks of stone prevented us from digging deep enough. So we were obliged to diminish the spacing between profiles to 10 cm to prepare them in sections without blocks. Nevertheless, only four profiles had the desired depth of about 1 m and were suitable for further analysis.

Image processing

The profiles were lit by halogen projectors, with the result that the colour temperature of the images differed from that of daylight. Therefore white balance was adjusted in Photoshop CS2 RAW-Converter (Adobe, 2005) via the grey scale. Then the photographs were corrected for perspective and radial distortion with the software PTGui (New House Internet Services B.V., 2005). Radial distortion is due to imperfections of the lens and was modelled by a fourth degree polynomial:

$$r_{src} = a r_{dest}^4 + b r_{dest}^3 + c r_{dest}^2 + (1 - a - b - c) r_{dest}, \qquad (1)$$

where r_{src} is the radius between a pixel and the centre of the original image (source, measured in pixels), and r_{dest} is the radius in the corrected image (destination, measured in pixels). The radii r_{src} and r_{dest} are scaled such that the value 1 corresponds to:

$$\frac{1}{2} \max (\text{width}, \text{height}), \qquad (2)$$

of the image. Parameters a, b and c are so-called lens parameters and can be adjusted in PTGui. Furthermore, the software

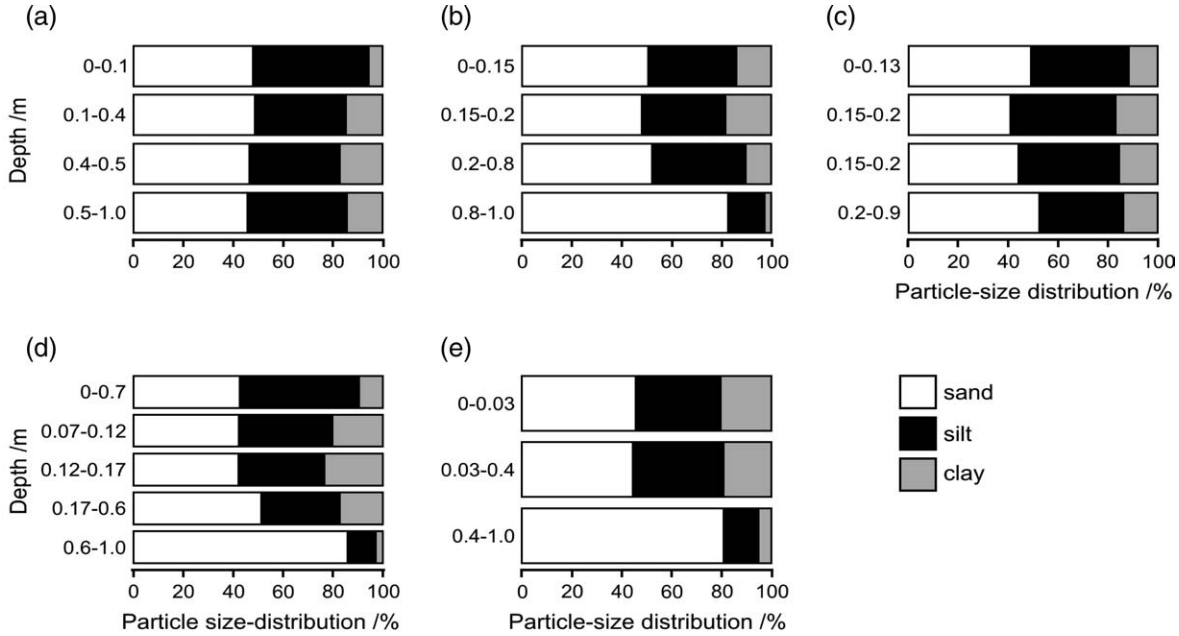

Figure 1 Particle-size distributions of the soil fine fraction on plots 1 (a) to 5 (e). Sand fraction is defined as 2000 – 63 μm, silt 63 – 2 μm and clay <2 μm. The different depth sections correspond to soil horizons.

PTLENS (Niemann, 2005) offers a data base of these values for many different types of cameras. Besides radial distortion, perspective distortion occurred because of rotation of the camera with respect to the photographed profile. We corrected it by setting control points all along the sides of the rectangular frame and adjusting them to horizontal and vertical lines. To decrease computing time, the image size was reduced such that 1 cm corresponded approximately to 6 pixels. This reduction did not affect further calculations as preliminary tests with different image resolutions had shown. In some images parts of the plot surfaces or shadows of the frame were visible. These regions would disturb further processing and were cut off. So the upper boundary of the output image corresponded to the first line in the photograph where the plot surface was no longer visible. Using MATLAB 7.1 (The MathWorks, Inc., 2005b) and the Image Processing Toolbox (The MathWorks, Inc., 2005a), we extracted the blue patterns from Brilliant Blue stained images by a colour-based segmentation by *k*-means clustering (MacQueen, 1967) in the CIE 1976 *L*a*b** colour space. Segmentation of iodine–starch patterns by *k*-means clustering algorithm was not good enough because the colour of the iodine–starch complex and that of the upper soil horizons were similar. Therefore we tried a classification based on hyper cuboids, an approach implemented in HALCON (MVTec Software GmbH, 2005). Finally, after segmentation, we generated binary images with stained parts in black and non-stained in white and calculated the dye coverage function $p(d)$ (the number of stained pixels per depth d).

Extreme value model

Schlather & Huwe (2005) proposed a method for quantitative analysis of images from dye tracer experiments based on extreme value theory (see Coles (2001), for an introduction). They applied the generalized Pareto distribution, a limit distribution of the extreme value theory with two parameters, to an idealized model of dye drops that run through soil along paths. The main idea is that the maximum depth z of a dye-stained path after n drops converges to the so-called *generalized extreme value distribution* (GEV), if $n \to \infty$ and the following assumptions as stated in Schlather & Huwe (2005) are satisfied:

'**1** any drop stains the path continuously up to the travel distance;

2 z is in the maximum domain of attraction of the generalised extreme value distributions (Resnick, 1987);

3 the travel distances of the drops are independent and identically distributed.'

Statement **2** means that the maxima of z become GEV distributed. Excesses below greater depths converge to the *generalized Pareto distribution H*:

$$H(d, \xi_r, s) = 1 - \left\{1 + \frac{\xi_r (d - D)}{s}\right\}^{-\frac{1}{\xi_r}}, \qquad (3)$$

where D is the threshold depth beyond which the data are assumed to follow closely the Pareto distribution, d is the profile depth (d and D are measured in pixels on a photograph, $d > D$), ξ_r is the form parameter ($\xi_r \in \mathbb{R}$) and s is the scale

parameter ($s > 0$), such that $(1 + \xi_r (d - D) /s) > 0$. Schlather & Huwe (2005) argued that the dye coverage function $p(d)$ is an estimate of the probability that a path is stained at least down to this depth, modulo a constant factor m. The distribution $1 - H$ is fitted to the normalized dye coverage function $p(d)/m$ and describes the conditional probability that a path is still stained to a depth d, given that it is stained to the depth D (for $d > D$). The form parameter ξ_r is defined as a risk index for vulnerability of groundwater to pollutants. Although the theoretical model describes drops travelling along distinct paths, Schlather & Huwe (2005) stated that it could be applied both to preferential and matrix flow. In the case of matrix flow, paths are replaced by micropaths and drops by infinitesimal volumes of dye (the terms 'micro' and 'infinitesimal' are used in the sense of Marshall *et al.* (1996)). So the model always describes the predominant flow regime.

In this study we slightly modified the interpretation of the risk index. We think that the form parameter of the generalized Pareto distribution should be interpreted as a risk index for vulnerability of groundwater to pollutants only in regions with fairly homogeneous geological material between the soil surface and the water table, as in sedimentary basins with shallow water tables. The groundwater at our site is 8–10 m below the surface, and so we prefer to qualify ξ_r as a risk index for vertical solute propagation.

The parameter ξ_r determines the form of the generalized Pareto distribution. If it is negative, the distribution has an upper end point, that is dye infiltration stops before attaining a certain depth and the dye coverage function reaches zero. In this case, there is a low risk of solute's propagating in greater depths. If ξ_r is positive then the distribution has no finite upper point, it decreases slowly and does not reach zero. Therefore the risk of solute propagation is high. Values of ξ_r around 0 describe a transition zone. The scale parameter s 'stretches' the distribution and can easily be interpreted for negative form parameters. Given a fixed negative ξ_r, s depends monotonically on the maximum infiltration depth, that is the deeper the maximum infiltration depth the larger the value of s. So for the same value of ξ_r, the risk of solute propagation increases with larger values of s (Figure 2). For positive form factors, s is difficult to measure in the field. But for a fixed positive ξ_r, the portion of the stained area in a certain depth is greater for larger values of s. Indeed, as s 'stretches' the distribution, larger values of $1 - H$, that is larger portions of stained pixels, can be found deeper in the soil.

Schlather & Huwe (2005) affirmed that the scale parameter s depends strongly on experimental conditions such as the amount of sprinkled tracer solution or the time between irrigation and excavation of profiles. The behaviour of the form parameter ξ_r under changing initial or experimental conditions is not clear, even though it seems to show some persistence against small variations.

For a reliable estimation of the risk index of a soil, Schlather & Huwe (2005) proposed taking at least 15 pictures. We used 28 pictures from five different experiments. Our goal was not to characterize the site but rather to understand the behaviour of the risk index under various initial and boundary conditions.

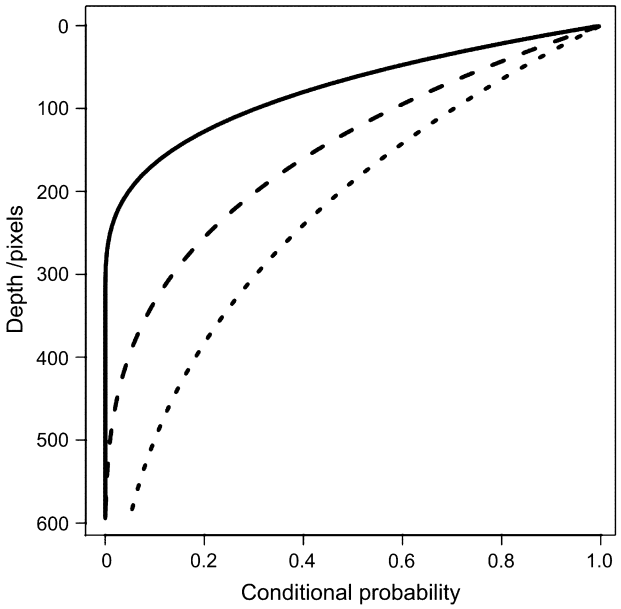

Figure 2 Effect of increasing values of scale parameter s on the probability distribution $1 - H$. Form parameter ξ_r is fixed to -0.3, scale parameter s equals 100 (solid line), 200 (dashed line) and 300 (dotted line), D equals 0.

Parameter estimation

As stated above, the generalized Pareto distribution describes excesses below greater depths, so we may not consider processes near the soil surface. We first estimated the parameter ξ_r and then s. The estimation of ξ_r is complex and recalls the ideas of Schlather & Huwe (2005) that are summarized in the following (see also the extension package SoPhy ver 1.0.25 (Schlather, 2005) of R (R Development Core Team, 2007)). Assume that we know the threshold D beyond which the data follow (approximately) the Pareto distribution. Then the parameter ξ_r and the parameter s can simultaneously be estimated by a non-linear parameter optimization, e.g. non-linear least squares or maximum likelihood. As we do not know D, ξ_r has to be estimated for a range of values of D. We might expect to get the same value of ξ_r for any D, except for some (small) error. This, however, is not true, and ideally $\xi_r(D)$ behaves as in the sketch in Figure 3.

The horizontal line designates the true value of ξ_r and the circles indicate the estimated values of ξ_r depending on the threshold depth D. Three areas of D can be distinguished, marked by the two vertical lines. The middle part gives the correct estimation of ξ_r. To the left, D is not large enough, so that we are outside the assumed asymptotics, that is the assumption that the data can be approximated by a Pareto

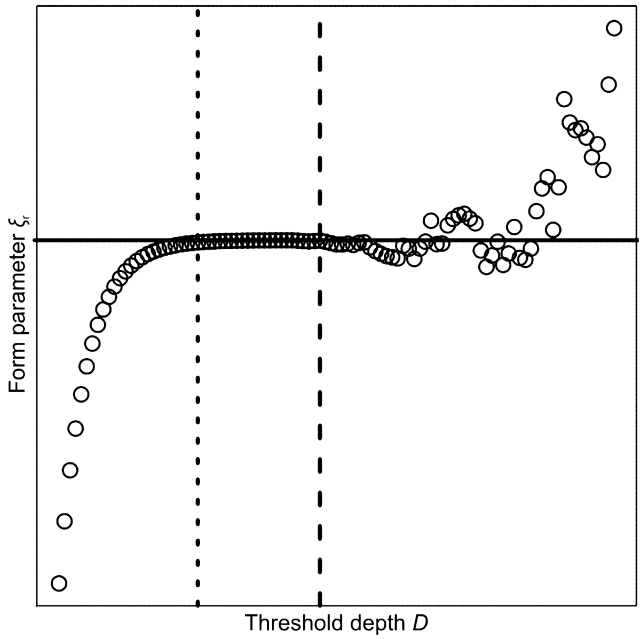

Figure 3 Schematic evaluation of the form parameter ξ_r with changing threshold depth D. The horizontal line designates the true value of ξ_r and the two vertical lines mark three areas of D: in the middle, ξ_r is correctly estimated; to the left, D is not large enough and the data cannot be approximated by a Pareto distribution; to the right, the number of data is small, so that larger variations in the estimation are visible.

distribution below such a threshold D is wrong. To the right, the number of data available below the (large) threshold of D is small, so that larger variations in the estimation are visible.

Schlather & Huwe (2005) aimed: (i) to find the middle part, (ii) to estimate ξ_r from the middle part, and (iii) to do it automatically. To achieve (iii) they suggested to take as middle part the values of D, where the maximum number of stained pixels of $p(d)$ ($d > D$) lies between 50 and 80%. For robustness, the median of the corresponding values of $\xi_r(D)$ is taken to get a final estimate for ξ_r. In contrast to ξ_r, the scale parameter will depend on D even under idealized conditions. Hence, we cannot get a final estimate for s in a similar way. Instead, we chose as the value of D the depth where $p(D)$ equalled 80%, and we estimated s in a next step whilst keeping ξ_r and D fixed. The maximum likelihood estimator is frequently used for fitting parameters, as it is possible to calculate confidence intervals because of its approximate normality (Coles, 2001). However, the maximum likelihood estimator did not behave well for our data, and so we preferred the least-squares estimator until a better estimator that provides confidence intervals is found.

For stratified soil as at our study site, to find the middle part to estimate ξ_r was more complex. The dye coverage functions were multimodal with a more or less pronounced second maximum in the lower soil (see Figure 4d, the first maximum is at the soil surface, the second one in about 130 pixels depth). So, following the proposition in Schlather & Huwe (2005), we applied the Pareto distribution only to the lowest part of the soil profile. Undocumented comparisons between different fitting procedures showed best results when we used the part of the dye coverage function where $p(d)$ lies between 0 and 80% of the number of stained pixels at its second maximum. We took the median of these values to calculate the final ξ_r. We estimated the scale parameter s in R (R Development Core Team, 2007) by unweighted non-linear least-squares regression using the form parameter ξ_r determined in SoPhy (Schlather, 2005) and taking the depth where $p(D)$ equals 80% of the number of stained pixels at the second maximum, as D. In forthcoming versions of SoPhy, the final estimation of the scale parameter s will be implemented. As a measure of goodness of fit, we calculated the coefficient of determination R^2 defined as

$$R^2 = 1 - \frac{\sum\{p(d) - \hat{p}(d)\}^2}{\sum\{p(d) - \bar{p}\}^2}, \quad (4)$$

where $p(d)$ is the number of stained pixels in the depth d ($d > D$), $\hat{p}(d)$ is the estimated number of stained pixels in the depth d and $\bar{p}$ is the mean number of stained pixels in the part of the profile used for fitting the $1 - H$ distribution. The coefficient of determination can be negative if the enumerator is larger than the denominator, that is if the chosen function fits the data worse than a vertical line through the mean of the data (Kvålseth, 1985).

Results

Qualitative analysis of flow patterns

In the following section we adopt the nomenclature proposed by Weiler & Flühler (2004) to describe flow processes based on the appearance of flow patterns. Figure 4 shows examples of binary images and their corresponding dye coverage functions. The soil profiles we excavated had a litter layer up to 10 cm thick and its first few centimetres were homogenously stained on all plots. The infiltration front broke into preferential paths in the lower part of the litter layer. Thus infiltration into the loamy upper soil (see Figure 1 for soil texture data) was inhomogeneous, and water flow bypassed large portions of the soil matrix in the upper 10–20 cm of the profiles. Accordingly, the dye coverage function decreased rapidly. In the upper soil, we found blue stained roots, indicating that there had been macropore flow in root channels.

The maximum of the dye coverage function was represented by large stained spots found between 20 and 40 cm. Texture analysis did not indicate any abrupt changes, but the root system was less dense. So one possible explanation is that macropore flow in root channels decreased and the flow regime changed to predominantly heterogeneous matrix flow. Further studies

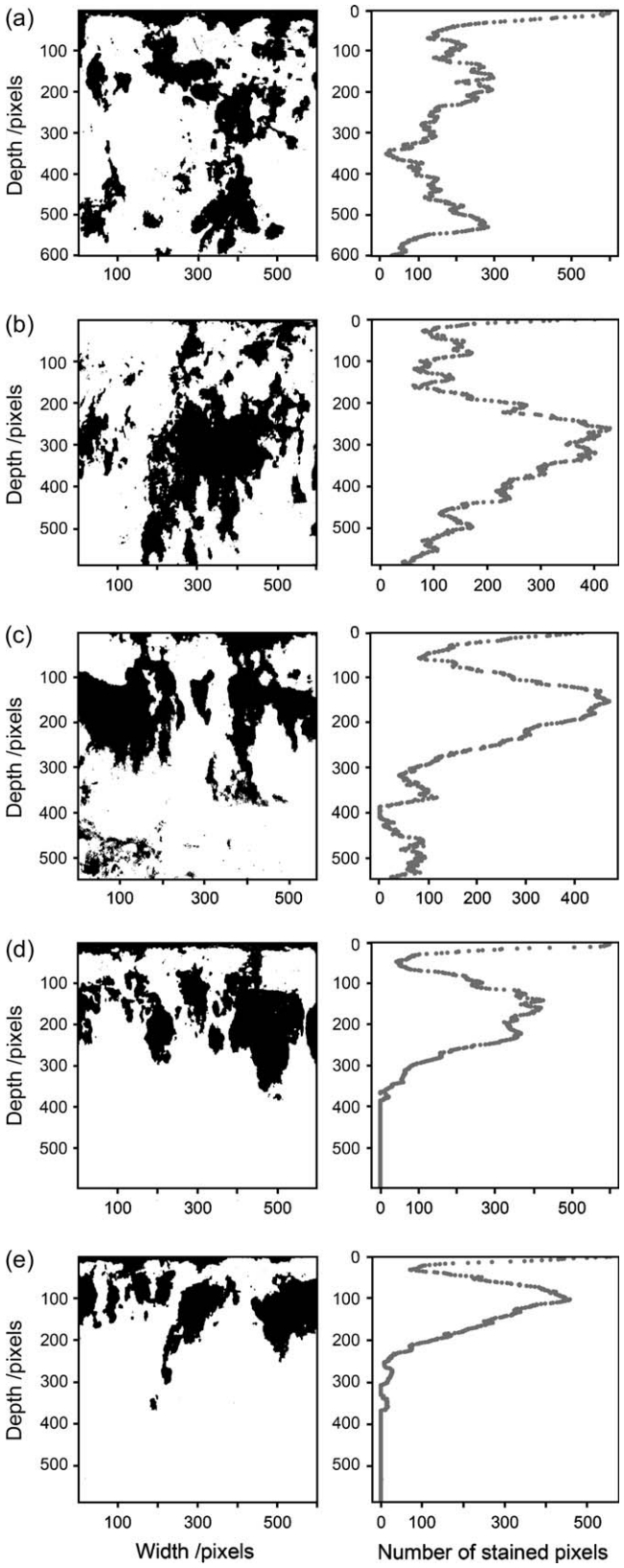

should investigate if the root system is really responsible for this transformation of flow regime.

In the lower soil, heterogeneous matrix flow and fingering dominated, but water flowed along macropores containing both dead and living roots when these were encountered. This was especially the case on plots 1 and 2. The exchange of water and solute between macropores and soil matrix was greater on 'moist' plots (1, 2 and 3) than on 'dry' plots (4 and 5). The effect of pre-irrigation on plot 2 supported this observation, because the stained spots on this plot were larger than on plot 1.

Plots 1, 2 and 3 were stained down to the bottom of the profile, that is 1 m, whereas on plots 4 and 5 dye infiltration stopped at between 70 and 80 cm. On plot 3 less dye infiltrated in greater depths than on plots 2 and 3, as indicated by a smaller portion of blue-stained surface. The surfaces of the stones in plot 3 served as preferential flow routes and were stained.

Figure 5 shows an example of Brilliant Blue and iodine–starch patterns on plot 4. In the upper 10 cm of the soil, there was no significant difference between the two tracers, neither in the location of the tracers inside the profile nor in the covered surface (see Figure 5, 0–40 pixels depth). But lower in the soil the iodine–starch spots were larger and the infiltration depth of iodide was greater than that of Brilliant Blue.

Two critical aspects remain when we compare the infiltration depths of Brilliant Blue and iodide. First, the redistribution time was different for Brilliant Blue and iodine–starch profiles, as the last were allowed to react overnight. Lu & Wu (2003) stated in their work that 1–2 hours of reaction are sufficient for the development of the iodine–starch complex. At our site the first colour reaction was visible after approximately 2 hours. So there was indeed fixation of iodide after only a few hours of reaction. Once fixed, iodide becomes much less mobile as the molecules of the iodine–starch complex are large. But the contrast to Brilliant Blue, especially in areas stained by both tracers, was too low, and therefore, the iodine–starch complex was allowed to develop overnight. Thus, even if there was a difference in redistribution times, it was less than 12 hours. Secondly, the minimum concentration still visible on a profile might be different for the two tracers, and so the actual infiltration depth could be greater.

Risk indices

In order to balance small fluctuations in the dye coverage function, we superposed all Brilliant Blue stained profiles of the same plot. Figure 6 shows these superposed profiles and the fitted distribution $1 - H$. Table 2 presents the risk indices ξ_r and the scale parameters s. To demonstrate the variations of the risk indices between profiles of one plot, minimum and maximum

Figure 4 Example images from dye tracer experiments on plots 1 (a) to 5 (e). Six pixels correspond to 1 cm. Left column: binary images from Brilliant Blue stained profiles with blue parts in black and non-stained regions in white. Right column: the corresponding dye coverage functions.

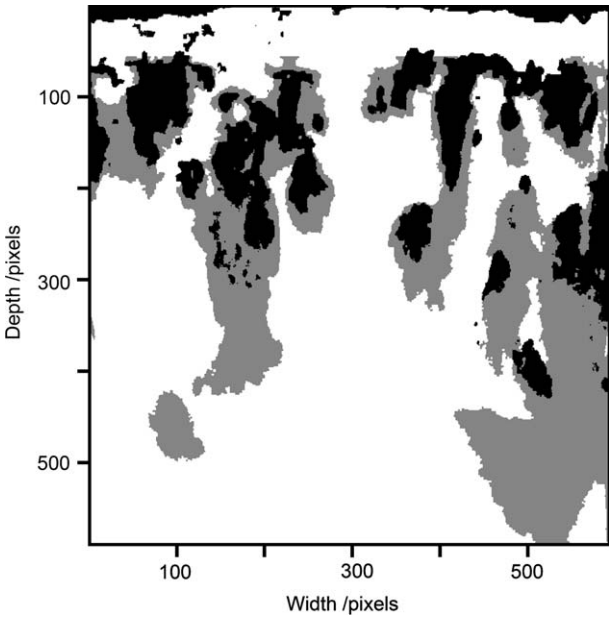

Figure 5 Example of Brilliant Blue (black) versus iodine–starch (grey) patterns on plot four. Six pixels correspond to 1 cm.

of estimates of ξ_r on single profiles are shown in the columns 'Minimum of ξ_r' and 'Maximum of ξ_r'. We used only single profiles where $1 - H$ was successfully fitted (visual check) and where R^2 exceeded 0.5 to calculate the minima and maxima.

Except on plot 3, the calculated risk indices are negative. It means that the dye infiltration will stop before reaching a certain depth. Thus there is a low risk of solute moving to greater depth below the analysed part of the profile. The risk index on plot 3 equals 0. Here, the dye coverage function decreases exponentially and does not reach 0, but the amount of dye carried to greater depth below the analysed profile might be negligible (Schlather & Huwe, 2005).

On plots 1 and 2, several Brilliant Blue profiles had a multimodal dye coverage function with two similar maxima in the lower soil (as in Figure 4a, depths 200 and 530 pixels, respectively), so even superposing them did not result in a monotonically decreasing function. Especially on plot 1, the third maximum appeared in the last third of the profile and led to a poor fit. One possible reason for this is the automated procedure to determine the starting point of the fit. Another reason is that the generalized Pareto distribution does not reflect flow processes in soils completely as the model theory is based on idealized assumptions. The distribution $1 - H$ is a monotonically decreasing function, and the quality of the fit depends strongly on the monotonicity of the dye coverage function. Therefore, the model is not suitable for dye coverage functions with pronounced multimodal behaviour as on plot 1.

We did not superpose iodine–starch stained profiles because there were too few. Risk indices based on these patterns were compared with those of Brilliant Blue of the same profile. The maximum difference in length between Brilliant Blue and iodine–starch profiles on the same plot was 26 pixels or 4 cm. Table 3 shows the results for profiles where $1 - H$ was successfully fitted (visual check) and where R^2 exceeded 0.5 for Brilliant Blue as well as for iodine–starch patterns.

Except on plot 3, where R^2 was small, risk indices ξ_r for iodine–starch are less than those for Brilliant Blue patterns, indicating a lower risk for propagation of iodide. This is in contradiction with the greater infiltration depth of this solute and is discussed below.

Discussion

Risk index for stratified soils

As mentioned by Schlather & Huwe (2005), especially in stratified soils with pronounced differences in physical properties between horizons, the application of the generalized Pareto distribution to several strata is problematic. At our study site, the stratification seems to be due to changes in root distribution between 20 and 40 cm depth. Macropore flow that starts in the upper soil ends as matrix flow in lower horizons with a less dense root system. When the flow process changes as a result of varying physical properties the dye coverage function cannot be represented by one single distribution $1 - H$. The evident solution is to use only the lowest part of the profile to fit the distribution as we did in our study. This accords with the limit law of the extreme value theory stating that the behaviour of the process at great depths is independent of the behaviour near the origin (Schlather & Huwe, 2005).

Furthermore, Schlather & Huwe (2005) stated in their paper that preferential flow is frequently linked to a positive risk index and matrix flow to a negative one. This is no longer true for stratified soils because only the lowest part of the profile is considered. At our study site, despite the occurrence of macropore flow in the upper soil, the calculated risk indices are negative, as the distribution $1 - H$ is fitted only to the lowest strata, and there the dominant flow regime is inhomogeneous matrix flow. So for correct assessment of risk of vertical solute propagation, the analysed profile depth should be taken into account.

Combination of form and scale parameters

Smaller risk indices for propagation of iodide are in contradiction with the greater infiltration depth of this solute. It is not surprising that the form parameter changes, as Brilliant Blue and iodide have different sorption characteristics. Especially in the lower soil where heterogeneous matrix flow and fingering dominated, Brilliant Blue was retarded with regard to iodide and their respective dye coverage functions differed in shape. We can resolve the contradiction by using both parameters, ξ_r and s, to estimate the risk of vertical solute propagation. As mentioned before, the scale parameter s 'stretches' the generalized Pareto distribution. So for the same risk index ξ_r the probability

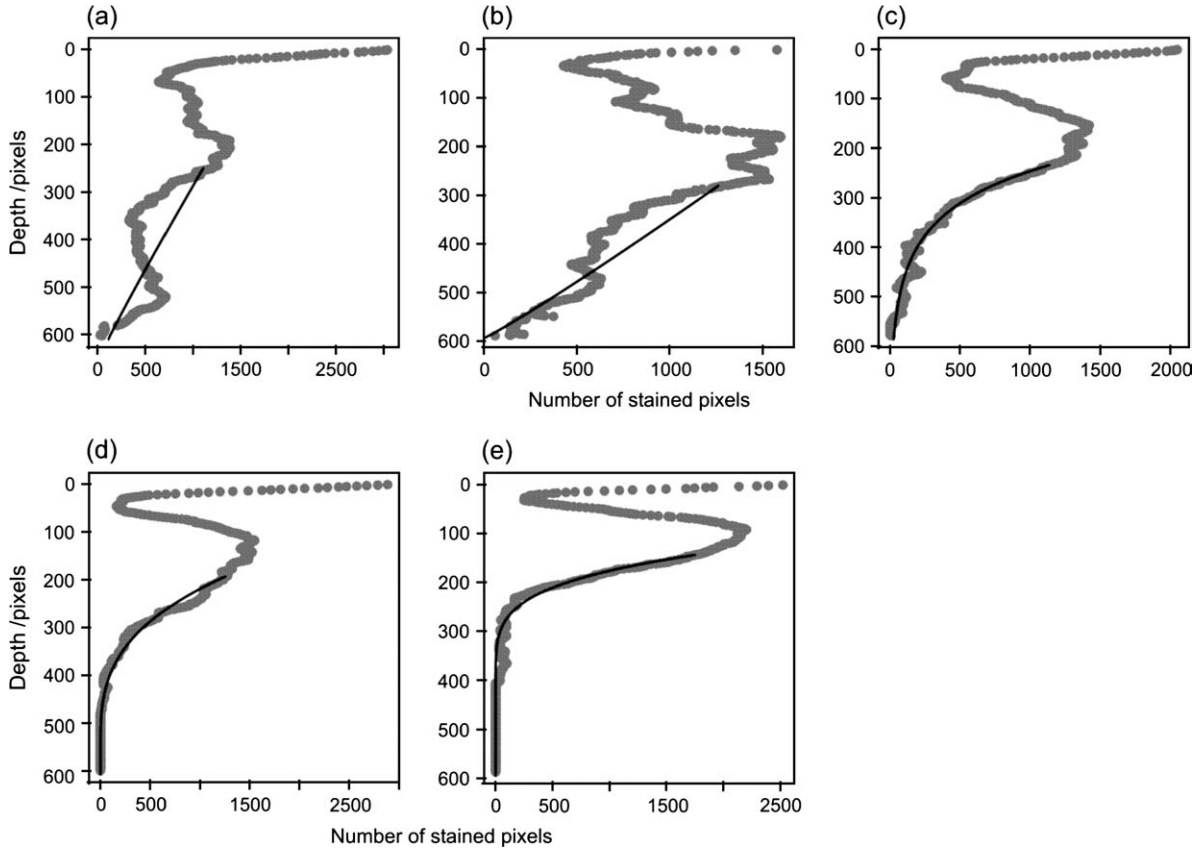

Figure 6 Dye coverage function of superposed profiles (dots) and fitted distribution $1 - H$ (line) on plot 1 (a) to plot 5 (e). Six pixels correspond to 1 cm.

to find stained pixels at a certain depth increases with larger values of s. The combination of ξ_r and s determines a complete probability distribution. Figure 7a shows the real difference between the risk of solute propagation based on Brilliant Blue (solid line) and iodine–starch patterns (dashed line) (see Figure 5 for patterns). The length of both profiles used for the adjustment of the generalized Pareto distribution differs by only 7 pixels (about 1 cm). The dashed line is situated right of the solid line, indicating a higher risk for iodide propagation.

Table 2 Calculated risk indices for superposed profiles

Plot	ξ_r	s	R^2	Minimum of ξ_r[a]	Maximum of ξ_r[a]
1	−0.9	377	−0.49[b]	0.4	1.3
2	−1.1	334	0.62	−1.0	0
3	0	94	0.99	0	0.1
4	−0.3	118	0.97	−0.9	0.0
5	−0.2	61	0.98	−0.1	0.5

[a]Minimum and maximum of ξ_r for single (not superposed) profiles show the variation of the risk index within the plot. Results are presented for profiles where $1 - H$ was successfully fitted (visual check) and where R^2 exceeded 0.5.

[b]A negative R^2 indicates that the adjusted curve fits the data worse than a vertical line through the mean value of the data.

The same procedure should be applied to assess the risk of Brilliant Blue propagation. Plots 4 and 5 are good examples. Here, the estimated risk indices are similar, but the scale parameters vary as predicted by Schlather & Huwe (2005) because of changing experimental and initial conditions. So the estimated actual risk of solute propagation is different on these plots. In Figure 7b we show the probability distributions $1 - H$ for the five superposed Brilliant Blue profiles (see Table 2 for parameters). For correct interpretation the fitted distributions are plotted for the part of the profile they were calculated for, that is beyond the threshold depth D. Despite the negative risk indices, it is clear that preferential flow is responsible for deep

Table 3 Risk indices for profiles with Brilliant Blue and iodide–starch patterns

	Brilliant blue			Iodide–starch		
Plot[a]	ξ_r	s	R^2	ξ_r	s	R^2
2	−0.9	46	0.85	−1.0	245	0.71
3	0.1	74	0.89	3.5	5	0.54
4	−0.5	159	0.87	−1.4	659	0.80
5	0	58	0.96	−0.9	261	0.96

[a]Adjustments on plot 1 did not give satisfying results.

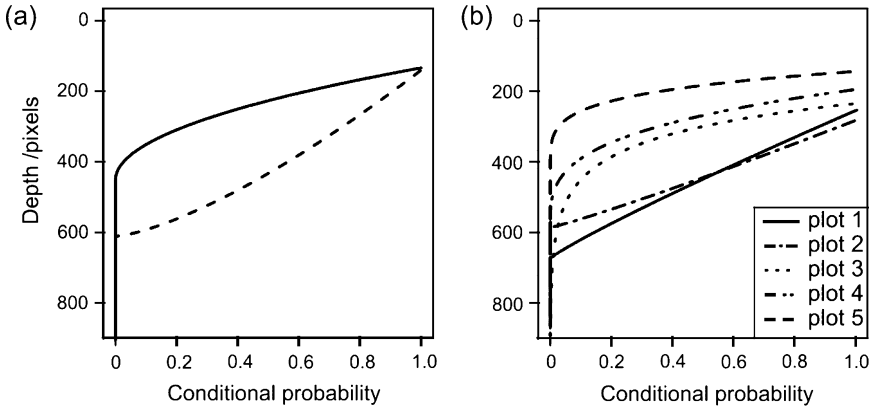

Figure 7 (a) Probability distribution for Brilliant Blue (solid line) and iodine–starch patterns (dashed line) on plot 4. (b) Probability distributions of the superposed Brilliant Blue stained profiles. The depth of the profiles is about 600 pixels, so in the case of plots 1, 2 and 3 the dye reached the bottom of the profile.

infiltration of the tracer. Based on our data, the estimated risk for solute propagation tends to increase from 'dry' to 'moist' plots.

Dependence of the risk index on boundary conditions

In our experiment, changing the irrigation intensity from 64 to 32 mm hour^{-1} seems to not affect the risk index significantly. Indeed, ξ_r on plot 4 was -0.3 and on plot 5 -0.2 (Table 2). But according to the theory, the scale parameter s changes (halves) as experimental conditions are modified. The combination of the two parameters indicates a higher risk of solute propagation on plot 4, that is for the higher irrigation rate.

It is more difficult to see the effect of pre-irrigation on plot 2 as the fit is unsatisfactory. Moreover, it cannot be compared with plot 1, which has similar initial moisture conditions because the distribution $1 - H$ could not be fitted properly on this plot either. But as indicated by the dye coverage function, the stained surface was larger on the pre-irrigated plot 2 than on plot 1. This would support the hypothesis that the initial soil moisture is an important factor. Compared with 'dry' plots 4 and 5, the risk index on plots 1 and 2 is lower, but s is much larger. The risk on plot 3 is the highest in accord with the highest initial moisture content. The tail of the distribution decreases exponentially ($\xi_r = 0$), and the dye penetrates deeper than on other plots. But as stated in Schlather & Huwe (2005), the transported mass might be negligible. Indeed, the dye-covered surface in the lower part of the profile is more important on plots 1 and 2 than on plot 3. So after combining ξ_r and s, the complete distribution $1 - H$ supports a higher risk of vertical solute propagation for moist initial conditions.

Actually, initial soil moisture seems to be a crucial factor. Dye coverage functions on 'moist' plots fluctuated more than on 'dry' ones, so the quality of the fit was poorer, especially for single profiles. More rapid flow velocities and interactions between preferential flow paths and a moister matrix are one possible explanation. Hence, flow patterns are more complex, and the resulting dye coverage functions do not decrease monotonically.

Finally, the risk index seems to depend on the tracer, but we need more data (iodine–starch stained profiles) to verify this. Although experimental and initial conditions for Brilliant Blue and iodide are the same, their risk indices and scale parameters tend to differ in the same profile. This phenomenon is probably due to different physical properties of the two tracers (especially their sorption behaviour) and is not a characteristic of the risk index.

Conclusions

We varied experimental and initial conditions for our tracer experiments and used two different tracers, Brilliant Blue and iodide, to study the behaviour of the risk index ξ_r. Our results support the hypothesis formulated by Schlather & Huwe (2005) that the risk index is to some degree invariant to changing experimental conditions (such as irrigation rate) and that the scale parameter s strongly depends on them. The initial soil moisture, however, seems to have a large influence on the risk index.

We propose to combine the two parameters of the generalized Pareto distribution to estimate the risk of vertical solute propagation in soils. The scale factor s reflects the maximum infiltration depth (for negative risk indices) or the amount of stained area at a certain depth (for positive risk indices). This information is important to assess correctly the risk and should be taken into account. Furthermore, a complete probability distribution $1 - H$ allows us to compare plots with different initial and experimental conditions or various tracers. For stratified soils, only the lowest part of the profile was used for the adjustment of the $1 - H$ distribution. Thus the depth should be explicitly included when one interprets the risk of vertical solute propagation.

To deal with strongly fluctuating or not decreasing dye coverage functions, the theory should be improved to account for tortuosity of flow paths. Provided that the dye coverage function decreases monotonically, the estimated risk for solute propagation can serve to classify soils. In stratified soils, different flow regimes can occur in different regions of the profile. To

assess the risk for vertical solute propagation the generalized Pareto distribution should be fitted to the lowest part of the soil profile. But it could possibly be applied to single horizons as well to characterize the various flow regimes within the profile. Further studies should help to identify homogenous zones of flow patterns corresponding to different flow regimes or reflecting different physical soil properties. Weiler & Flühler (2004), for instance, proposed an interesting classification approach using stereology. Applied to such homogenous zones, fitting results of the distribution $1 - H$ could be improved.

Acknowledgements

We thank Andreas Kolb and Iris Schmiedinger for their assistance during field and laboratory work, Tobias Zuber for providing data of soil matric potential and Professor Foken for the precipitation data. We also thank the reviewers for their scrutiny of our script and suggestions for improving it, and MVTec for providing a research-license for the software HALCON. This project was financially supported by the Deutsche Forschungsgemeinschaft (DFG FOR 562).

References

Adobe 2005. *Photoshop Version CS2* [WWW document]. URL http://www.adobe.com [accessed on November 2005].

Aeby, P., Forrer, J., Steinmeier, C. & Flühler, H. 1997. Image analysis for determination of dye tracer concentrations in sand columns. *Soil Science Society of America Journal*, **61,** 33–35.

Bowman, R.S. 1984. Evaluation of some new tracers for soil-water studies. *Soil Science Society of America Journal*, **48,** 987–993.

Coles, S. 2001. *An Introduction to Statistical Modeling of Extreme Values*. Springer-Verlag, London.

Farenhorst, A., Topp, E., Bowman, B.T. & Tomlin, A.D. 2000. Earthworm burrowing and feeding activity and the potential for atrazine transport by preferential flow. *Soil Biology and Biochemistry*, **32,** 479–488.

Flury, M. & Flühler, H. 1994. Brilliant blue FCF as a dye tracer for solute transport studies – a toxicological overview. *Journal of Environmental Quality*, **23,** 1108–1112.

Flury, M. & Wai, N.N. 2003. Dyes as tracers for vadose zone hydrology. *Reviews of Geophysics*, **41,** 2-1–2-37.

Flury, M., Flühler, H., Jury, W.A. & Leuenberger, J. 1994. Susceptibility of soils to preferential flow of water: a field study. *Water Resources Research*, **30,** 1945–1954.

Forrer, I.E., Kasteel, R., Flury, M. & Flühler, H. 1999. Longitudinal and lateral dispersion in an unsaturated field soil. *Water Resources Research*, **35,** 3049–3060.

Forrer, I.E., Papritz, A., Kasteel, R., Flühler, H. & Luca, D. 2000. Quantifying dye tracers in soil profiles by image processing. *European Journal of Soil Science*, **51,** 313–322.

German-Heins, J. & Flury, M. 2000. Sorption of brilliant blue FCF in soils as affected by pH and ionic strength. *Geoderma*, **97,** 87–101.

Ghodrati, M., Ernst, F.F. & Jury, W.A. 1990. Automated spray system for application of solutes to small field plots. *Soil Science Society of America Journal*, **54,** 287–290.

Gish, T.J., Kung, K.-J.S., Perry, D.C., Posner, J., Bubenzer, G., Helling, C.S. *et al*. 2004. Impact of preferential flow at varying irrigation rates by quantifying mass fluxes. *Journal of Environmental Quality*, **33,** 1033–1040.

Hendrickx, J.M.H., Dekker, L.W. & Boersma, O.H. 1993. Unstable wetting fronts in water-repellent field soils. *Journal of Environmental Quality*, **22,** 109–118.

Kasteel, R., Vogel, H.-J. & Roth, K. 2002. Effect of non-linear adsorption on the transport behaviour of brilliant blue in a field soil. *European Journal of Soil Science*, **53,** 231–240.

Ketelsen, H. & Meyer-Windel, S. 1999. Adsorption of brilliant blue FCF by soils. *Geoderma*, **90,** 131–145.

Kulli, B., Gysi, M. & Flühler, H. 2003. Visualizing soil compaction based on flow pattern analysis. *Soil and Tillage Research*, **70,** 29–40.

Kvålseth, T.O. 1985. Cautionary note about R^2. *American Statistician*, **39,** 279–285.

Lawes, J.B., Gilbert, J.H. & Warrington, R. 1882. *On the Amount and Composition of the Rain and Drainage Water Collected at Rothamsted*. Williams, Clowes & Sons, London.

Lu, J. & Wu, L. 2003. Visualizing bromide and iodide water tracer in soil profiles by spray methods. *Journal of Environmental Quality*, **32,** 363–367.

MacQueen, J.B. 1967. Some methods for classification and analysis of multivariate observations. In: *Proceedings of the 5th Berkeley Symposium on Mathematical Statistics and Probability*, Volume I (eds L. M. Le Cam & J. Neyman), pp. 281–297. University of California Press, Berkeley, CA.

Marshall, T.J., Holmes, J.W. & Rose, C.W. 1996. *Soil Physics*. Cambridge University Press, Cambridge.

Mitchell, A.R., Ellsworth, T.R. & Meek, B.D. 1995. Effect of root systems on preferential flow in swelling soil. *Communications in Soil Science and Plant Analysis*, **26,** 2655–2666.

Mon, J., Flury, M. & Harsh, J.B. 2006. Sorption of four triarylmethane dyes in a sandy soil determined by batch and column experiments. *Geoderma*, **133,** 217–224.

Morris, C. & Mooney, S.J. 2004. A high-resolution system for the quantification of preferential flow in undisturbed soil using observations of tracers. *Geoderma*, **118,** 133–143.

MVTec Software GmbH 2005. *Halcon Version 7.1* [WWW document]. URL http://www.mvtec.com/halcon/ [accessed on March 2006].

New House Internet Services B.V. 2005. *PTGui Version 5.5* [WWW document]. URL http://www.ptgui.com/ [accessed on February 2005].

Niemann, T. 2005. *PTLens Version 6.4* [WWW document]. URL http://epaperpress.com/ptlens/ [accessed on February 2005].

Öhrström, P., Persson, M., Albergel, J., Zante, P., Nasri, S., Berndtsson, R. *et al*. 2002. Field-scale variation of preferential flow as indicated from dye coverage. *Journal of Hydrology*, **257,** 164–173.

R Development Core Team 2007. *R: A Language and Environment for Statistical Computing. R Foundation for Statistical Computing, Vienna* [WWWdocument]. URL http://www.R-project.org [accessed on January 2007].

Resnick, S.I. 1987. *Extreme Values, Regular Variation, and Point Processes*. Springer, New York.

Ritsema, C.J. & Dekker, L.W. 2000. Preferential flow in water repellent sandy soils: principles and modeling implications. *Journal of Hydrology*, **231,** 308–319.

Schlather, M. 2005. *SoPhy: Some Soil Physics Tools for R* [WWW document]. URL http://www.r-project.org/, contributed extension package [accessed on January 2006].

Schlather, M. & Huwe, B. 2005. A risk index for characterising flow pattern in soils using dye tracer distributions. *Journal of Contaminant Hydrology*, **79,** 25–44.

Schumacher, W. 1864. *Die Physik des Bodens in ihren theoretischen und praktischen Beziehungen zur Landwirtschaft*. Wiegandt und Hempel, Berlin.

Shuster, W.D., Subler, S. & McCoy, E.L. 2002. The influence of earthworm community structure on the distribution and movement of solutes in a chisel-tilled soil. *Applied Soil Ecology*, **21,** 159–167.

The MathWorks, Inc 2005a. *Image Processing Toolbox Version. 5.1* [WWW document]. URL http://www.mathworks.com/products/image/ [accessed on July 2005].

The MathWorks, Inc 2005b. *Matlab version. 7.1* [WWW document]. URL http://www.mathworks.com [accessed on July 2005].

Vogel, H.-J., Cousin, I., Ippisch, O. & Bastian, P. 2006. The dominant role of structure for solute transport in soil: experimental evidence and modelling of structure and transport in a field experiment. *Hydrology and Earth System Sciences*, **10,** 495–506.

Wang, Z., Wu, Q.J., Wu, L., Ritsema, C.J., Dekker, L.W. & Feyen, J. 2000. Effects of soil water repellency on infiltration rate and flow instability. *Journal of Hydrology*, **231,** 265–276.

Weiler, M. & Flühler, H. 2004. Inferring flow types from dye patterns in macroporous soils. *Geoderma*, **120,** 137–153.

Weiler, M. & Naef, F. 2003. An experimental tracer study of the role of macropores in infiltration in grassland soils. *Hydrological Processes*, **17,** 477–493.